Thermal Equilibrium of the Atmosphere with a Given Distribution of Relative Humidity

Syukuro Manabe and Richard T. Wetherald

Geophysical Fluid Dynamics Laboratory, ESSA, Washington, D. C.

(Manuscript received 2 November 1966)

ABSTRACT

Radiative convective equilibrium of the atmosphere with a given distribution of relative humidity is computed as the asymptotic state of an initial value problem.

The results show that it takes almost twice as long to reach the state of radiative convective equilibrinm for the atmosphere with a given distribution of relative humidity than for the atmosphere with a given distribution of absolute humidity.

Also, the surface equilibrium temperature of the former is almost twice as sensitive to change of various factors such as solar constant, CO_2 content, O_3 content, and cloudiness, than that of the latter, due to the adjustment of water vapor content to the temperature variation of the atmosphere.

According to our estimate, a doubling of the CO_2 content in the atmosphere has the effect of raising the temperature of the atmosphere (whose relative humidity is fixed) by about 2C. Our model does not have the extreme sensitivity of atmospheric temperature to changes of CO_2 content which was adduced by Möller.

1. Introduction

This study is a continuation of the previous study of the thermal equilibrium of the atmosphere with a convective adjustment which was published in the Journal of the Atmospheric Sciences (Manabe and Strickler, 1964). Hereafter, we shall identify this study by M.S. In M.S. the vertical distribution of absolute humidity was given for the computation of equilibrium temperature, and its dependence upon atmospheric temperature was not taken into consideration. However, the absolute humidity in the actual atmosphere strongly depends upon temperature. Fig. 1 shows the distribution of relative humidity as a function of latitude and height for summer and winter. According to this figure, the zonal mean distributions of relative humidity of two seasons closely resemble one another, whereas those of absolute humidity do not. These data suggest that, given sufficient time, the atmosphere tends to restore a certain climatological distribution of relative humidity responding to the change of temperature. If the moisture content of the atmosphere depends upon atmospheric temperature, the effective height of the source of outgoing long-wave radiation also depends upon atmospheric temperature. Given a vertical distribution of relative humidity, the warmer the atmospheric temperature, the higher the effective source of outgoing radiation. Accordingly, the dependence of the outgoing long-wave radiation is less than that to be expected from the fourth-power law of Stefan-Boltzman. Therefore, the equilibrium temperature of the atmosphere with a fixed relative humidity depends more upon the solar constant or upon ab-

sorbers such as CO_2 and O_3, than does that with a fixed absolute humidity, in order to satisfy the condition of radiative convective equilibrium. In this study, we will repeat the computation of radiative convective equilibrium of the atmosphere, this time for an atmosphere with a given distribution of relative humidity instead of that for an atmosphere with a given distribution of absolute humidity as was carried out in M.S.

As we stated in M.S., and in the study by Manabe and Möller (1961), the primary objective of our study of radiative convective equilibrium is the incorporation of radiative transfer into the general circulation model
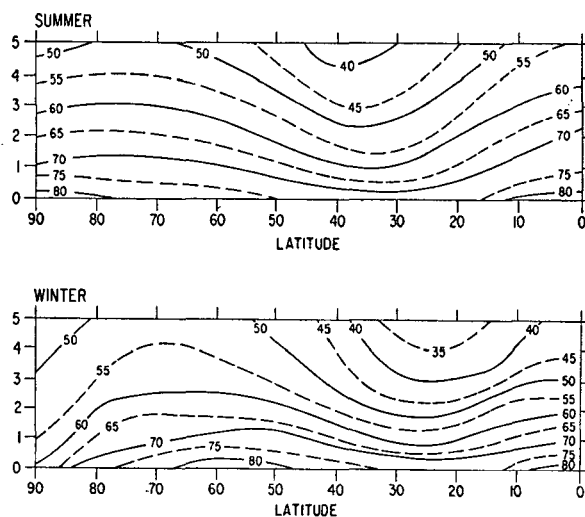

Fig. 1. Latitude-height distribution of relative humidity for both summer and winter (Telegadas and London, 1954).

of the atmosphere. Adopting the scheme of the computation of radiative transfer which was developed in M.S., Manabe *et al.* (1965) successfully performed the numerical integration of the general circulation of the atmosphere involving the hydrologic cycle. In order to avoid a substantial increase in the number of degrees of freedom, the distribution of water vapor, which emerged as the result of the hydrologic cycle of the model atmosphere, was not used for the computation of radiative transfer. Instead, the climatological distribution of absolute humidity was used. The next step is the numerical integration of the model with complete coupling between radiative transfer and the hydrologic cycle. Before undertaking this project, it is desirable to answer the following questions by performing a series of computations of radiative-convective equilibrium of the atmosphere with fixed relative humidity.

1) How long does it take to reach a state of thermal equilibrium when the atmosphere maintains a realistic distribution of relative humidity that is invariant with time?

2) What is the influence of various factors such as the solar constant, cloudiness, surface albedo, and the distributions of the various atmospheric absorbers on the equilibrium temperature of the atmosphere with a realistic distribution of relative humidity?

3) What is the equilibrium temperature of the earth's surface corresponding to realistic values of these factors?

There is no doubt that this information is indispensable for the successful integration of the fundamental model of the general circulation mentioned above.

Recently, Möller (1963) discussed the influence of the variation of CO_2 content in the atmosphere on the magnitude of long-wave radiation at the earth's surface,

and on the equilibrium temperature of the earth's surface. Assuming that the absolute humidity is independent of the atmospheric temperature, he obtained an order-of-magnitude dependence of equilibrium temperature upon CO_2 content similar to those obtained by Plass (1956), Kondratiev and Niilisk (1960), and Kaplan (1960). However, he obtained an extremely large dependence for a certain range of temperature when he assumed that relative humidity (instead of absolute humidity) of the atmosphere was given. One shortcoming of this study is that the conclusion was drawn from the computation of the heat balance of earth's surface instead of that of the atmosphere as a whole. Therefore, it seems to be highly desirable to re-evaluate this theory, using as a basis the computation of radiative convective equilibrium of the atmosphere with a fixed relative humidity. The results are presented in this study.

2. Radiative convective equilibrium

a. Description of the model. As we explained in the previous paper and in the introduction, the radiative convective equilibrium of the atmosphere with a given distribution of relative humidity should satisfy the following requirements:

1) At the top of the atmosphere, the net incoming solar radiation should be equal to the net outgoing long-wave radiation.

2) No temperature discontinuity should exist.

3) Free and forced convection, and mixing by the large-scale eddies, prevent the lapse rate from exceeding a critical lapse rate equal to 6.5C km^{-1}.

4) Whenever the lapse rate is subcritical, the condition of local radiative equilibrium is satisfied.

5) The heat capacity of the earth's surface is zero.

6) The atmosphere maintains the given vertical distribution of relative humidity (new requirement).

COMPUTATION OF THE MIXING RATIO OF WATER VAPOR, r^τ

$r = .622 \cdot h \cdot e_s(T)/(p - h \cdot e_s(T))$

COMPUTATION OF MEAN EMISSIVITY AND ABSORPTIVITY

CONVECTIVE ADJUSTMENT

COMPUTATION OF TEMPERATURE CHANGE DUE TO RADIATION

$\left(\frac{\partial T_I}{\partial t}\right)_R^\tau$

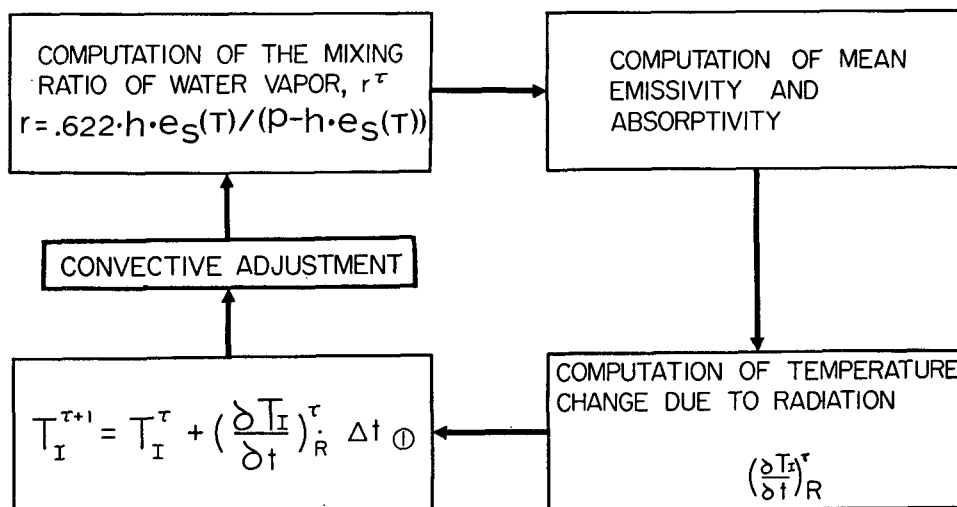$T_I^{\tau+1} = T_I^\tau + \left(\frac{\partial T_I}{\partial t}\right)_R^\tau \Delta t$ ①

FIG. 2. Flow chart for the numerical time integration.

In the actual computation, the state of radiative convective equilibrium is computed as an asymptotic state of an initial value problem. Details of the procedure are described in Appendix 1. The flow chart of the marching computation is shown in Fig. 2. In this figure $e_s(T)$ denotes the saturation vapor pressure of water vapor as a function of temperature T, and h denotes the relative humidity. τ denotes the number of the time steps of numerical integration, and I is the indexing of the finite differences in the vertical direction. (Refer to Appendix 3 for the illustration of levels adopted for vertical differencing.) The exact definitions of mean emissivity and mean absorptivity are also given in M.S., pp. 365–366.

Since the changes of absolute humidity correspond to the change of air temperature, the equivalent heat capacity of moist air with relative humidity h may be defined as

$$C_p' = C_p\left[1 + \frac{L}{C_p}\cdot\frac{\partial}{\partial T}\left(\frac{0.622he_s(T)}{p - he_s(T)}\right)\right], \quad (1)$$

where L and C_p are the latent heat of evaporation and the specific heat of air under constant pressure, respectively. The second term in the bracket appears due to the change of latent energy of the air.

The reader should refer to M.S. for the following information.

1) Computation of the flux of long-wave radiation.
2) Computation of the depletion of solar radiation.
3) Determination of mean absorptivity and emissivity.

Some additional explanation of how we determine the absorptivity is given in Appendix 2.

b. Standard distribution of atmospheric absorbers. In this subsection, the vertical distributions of water vapor, carbon dioxide, ozone, and cloud, which are used for the computations of thermal equilibrium, and those of heat balance in the following section, are described. They are adopted unless we specify otherwise.

The typical vertical distribution of relative humidity can be approximated with the help of the data in Fig. 3. In this figure, the hemispheric mean of relative humidity obtained by Telegadas and London (1954) and that of relative humidity obtained by Murgatroyd (1960) are shown in the upper and lower troposphere, respectively. The stratospheric distributions of relative humidity obtained by Mastenbrook (1963) at Minneapolis and Washington, D. C., are also plotted after some smoothing of data. Referring to this figure, the following linear function is chosen to represent the vertical distribution of relative humidity, i.e.,

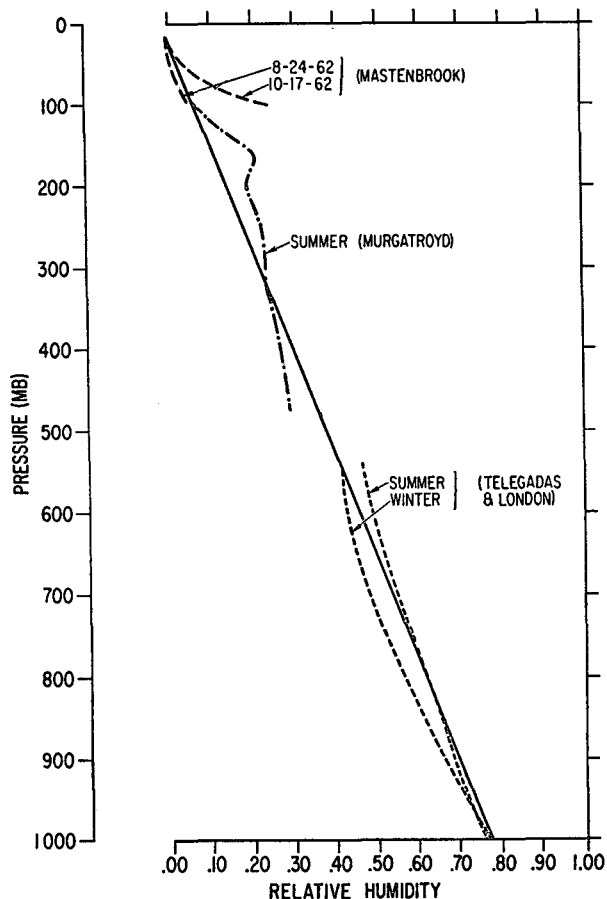$$h = h_*\left(\frac{Q - 0.02}{1 - 0.02}\right), \quad (2)$$

FIG. 3. Vertical distribution of relative humidity (Mastenbrook, 1963; Murgatroyd, 1960; Telegadas and London, 1954).

where h_* is the relative humidity at the earth's surface, equal to 0.77, $Q = p/p_*$, and p_* is surface pressure. When Q is smaller than 0.02, Eq. (2) gives negative value of h. Therefore, it is necessary to specify the humidity distribution for small Q values. According to the measurements by Mastenbrook (1963) and Houghton (1963), the stratosphere is very dry and its mixing ratio is approximately 3×10^{-6} gm gm^{-1} of air. We have therefore assumed that the minimum value of mixing ratio r_{min} to be 3×10^{-6} gm gm^{-1} of air, i.e., if

$$r(T,h)\left(= \frac{0.622he_s(T)}{p - he_s(T)}\right) < r_{min}, \quad (3)$$

set

$$r = r_{min}(= 3 \times 10^{-6} \text{ gm gm}^{-1} \text{ of air}).$$

The mixing ratio of carbon dioxide in the atmosphere is assumed to be constant. The mixing ratio adopted for the present computation is 0.0456% by weight (300 ppm by volume).

The vertical distribution of ozone which is used for the computation is shown in Fig. 4. This data is obtained by Herring and Borden (1965) using chemiluminescent ozonesondes for the period September
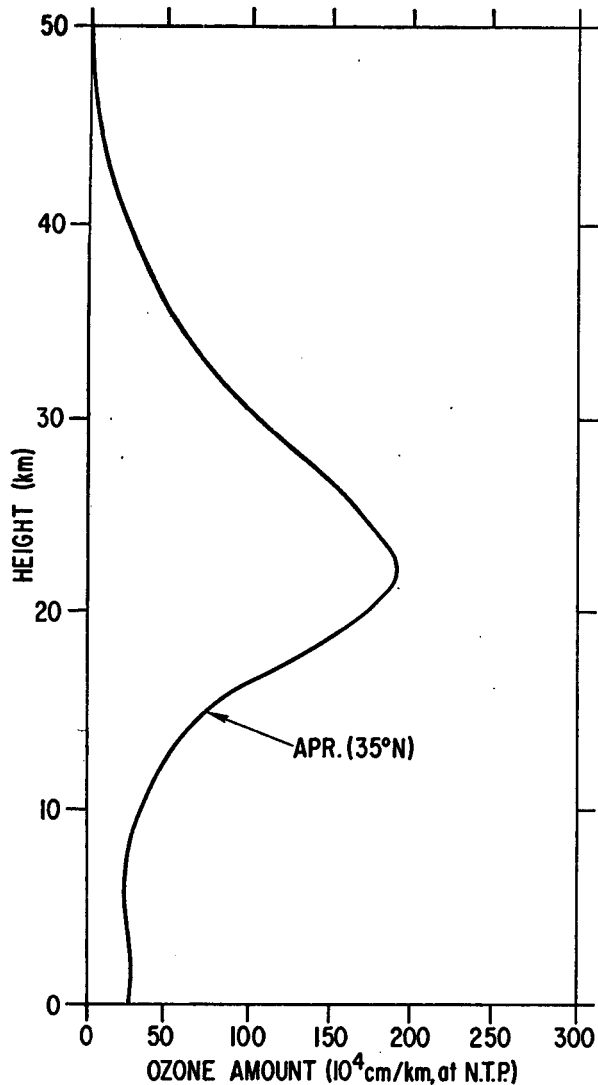
FIG. 4. Vertical distribution of ozone at 35N, April (Herring and Borden, 1965), normalized by the total amount from London (1962).

1963 to August 1964. The vertical distribution at 35N, April, is taken from the figure of his paper, and is normalized to the total amount of ozone obtained by London (1962).

The heights, albedo, and the amounts of cloud adopted for the computation are tabulated in Table 1. The albedo of the earth's surface is assumed to be 0.102.

TABLE 1. Cloud characteristics employed in radiative convective equilibrium model.

Cloud	Height (km)	Amount	Albedo
High	10.0	0.228	0.20
Middle	4.1	0.090	0.48
Low			
top	2.7	0.313	0.69
bottom	1.7		

c. *Hergesell's problem and radiative convective equilibrium.* Before discussing the results of the study of radiative convective equilibrium in detail, we shall briefly discuss the problem of pure radiative equilibrium (no convection) of the atmosphere with a given distribution of relative humidity. This problem was first investigated by Hergesell (1919) who criticized Emden's solution of pure radiative equilibrium because it allows a layer of supersaturation. Using the assumption of grey body radiation, he obtained, numerically, the state of pure radiative equilibrium of the atmosphere with a realistic distribution of relative humidity. The atmosphere in pure radiative equilibrium thus obtained is almost isothermal, and its temperature is extremely low due to the self-amplification effect of water vapor on the equilibrium temperature of the atmosphere. (For example, since the water content of the atmosphere decreases with decreasing temperature, the greenhouse effect of the atmosphere decreases, and so on.) Fig. 5 shows the solution of this problem which is obtained by our method without using the assumption of grey body radiation (cloudiness = 0). Although the surface equilibrium temperature is much higher than that obtained by Hergesell due to the effect of line center absorption, a sharp decrease of temperature with increasing altitude appears near the ground, and the temperature of the troposphere is much lower than that which is obtained for the atmosphere with a
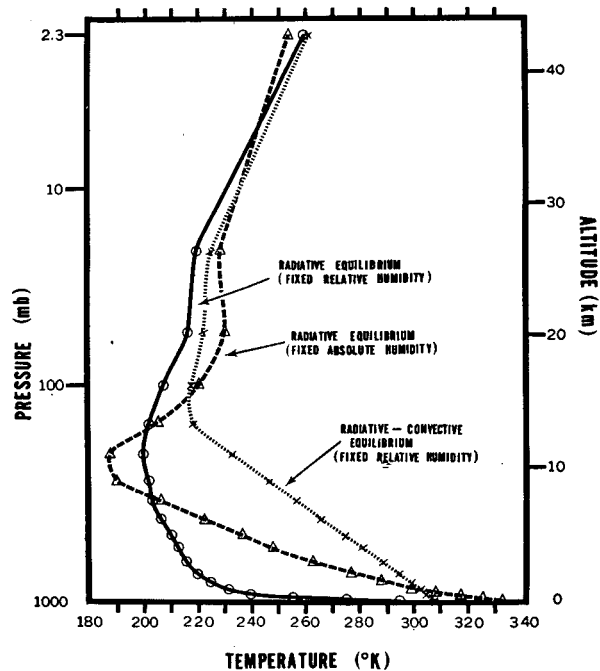

FIG. 5. Solid line, radiative equilibrium of the clear atmosphere with the given distribution of relative humidity; dashed line, radiative equilibrium of the clear atmosphere with the given distribution of absolute humidity; dotted line, radiative convective equilibrium of the atmosphere with the given distribution of relative humidity.
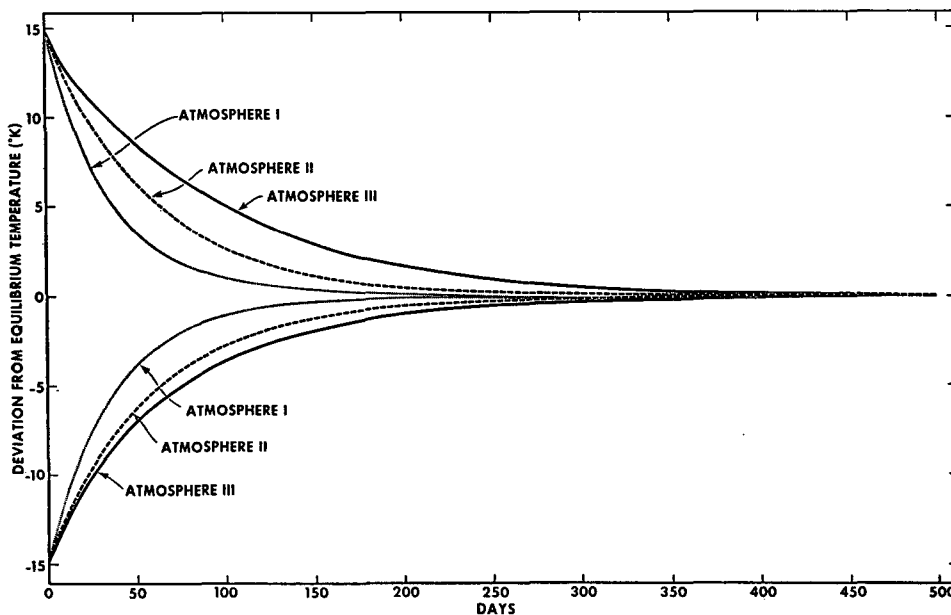
FIG. 6. Approach of vertical mean temperature toward the state of equilibrium. Atmosphere I
(dotted line), Atmosphere II (dashed line), Atmosphere III (solid line).

realistic distribution of absolute humidity. This is shown in the same figure. For the sake of comparison, the distribution of equilibrium temperature with convective adjustment is also shown in the figure. The distribution of humidity adopted for this computation is given by Eqs. (2) and (3).

This comparison clearly demonstrates the role of convective adjustment in maintaining the existing distribution of atmospheric temperature. Without this effect, the temperature of the troposphere as well as the height of the tropopause would have been unrealistically low due to the positive feedback effect of water vapor on the air temperature, which we discussed in the introduction.

d. Approach towards the equilibrium state. It should take longer for the atmosphere with a given distribution of relative humidity than for the atmosphere with a given distribution of absolute humidity to reach the state of thermal equilibrium. Two of the reasons for this difference are as follows:

1) As we explained in the introduction, the dependence of outgoing radiation of the atmosphere with a given distribution of relative humidity depends less on the atmospheric temperature than does that of an atmosphere with a given distribution of absolute humidity. Accordingly, the speed of approach towards the equilibrium state is significantly less.

2) Since the vertical distribution of relative humidity is constant throughout the course of the time integration, absolute humidity depends upon the atmospheric temperature, and the variation of absolute humidity involves the variation of the latent energy of the air. Therefore, the effective heat capacity of the air with

the given relative humidity is larger than the heat capacity of dry air. Accordingly, the speed of approach is slower.

In Fig. 6, the approaches of each of three idealized atmospheres towards the equilibrium are shown. These are as follows:

Atmosphere I: Vertical distribution of absolute humidity is constant with time.

Atmosphere II: Vertical distribution of relative humidity is constant with time. The heat capacity of the air is assumed to be 0.24 cal gm^{-1}, i.e., the heat capacity of dry air.

Atmosphere III: Vertical distribution of relative humidity is constant with time. The effective heat capacity of air which is given by Eq. (1) is adopted.

Two initial conditions which are chosen for the time integrations shown in Fig. 6 are obtained by adding 15K to the temperature distribution of radiative convective equilibrium.

Because of the first of the two reasons mentioned above, it takes about 1.5 times longer for Atmosphere II than for Atmosphere I to reach the state of equilibrium; and it takes even longer for Atmosphere III to reach equilibrium due to the second reason described above. In short, "the radiation-condensation relaxation" is much slower than pure radiation relaxation. Therefore, it is probable that the radiation-condensation relaxation is one of the important factors in determining the seasonal variation of atmospheric temperature. Also, Fig. 6 shows that it takes longer for the warm atmosphere to reach the state of equilibrium than for the cold atmosphere. This result suggests that
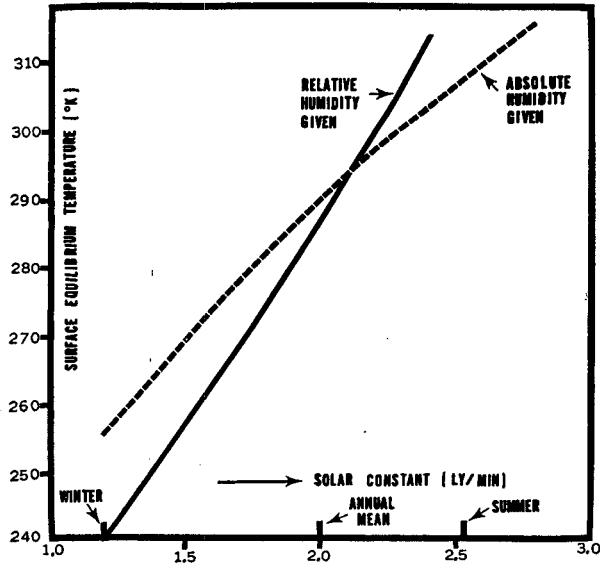
FIG. 7. Solar constant and surface temperature of radiative convective equilibrium. Solid line and dashed line show the case of fixed relative humidity and that of fixed absolute humidity, respectively. Insolation of summer and that of winter is obtained by taking the mean value for the period of June–July–August, and that of December–January–February.
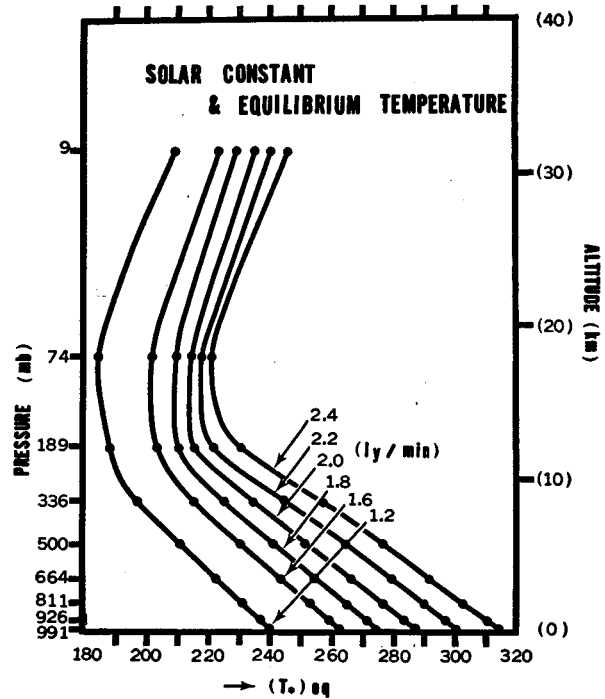

FIG. 8. Vertical distribution of radiative convective equilibrium temperature of the atmosphere with a given distribution of relative humidity for various values of the solar constant.

it is not advisable to perform the numerical integration of the general circulation model by starting from the very warm initial condition.

3. Solar constant and radiative convective equilibrium

a. Thermal equilibrium for various solar constants. One of the most fundamental factors which determines the climate of the earth is the solar constant. In order to evaluate the effect of the solar constant upon the climate of the earth's surface, a series of computations of thermal equilibrium was performed. Fig. 7 shows the dependence of the surface equilibrium temperature upon the solar constant for both the atmosphere with a given distribution of relative humidity, and that with a given distribution of absolute humidity.

According to this figure, the equilibrium temperature of the atmosphere with a given distribution of relative humidity is twice as sensitive to the change of the solar constant as that with a given distribution of absolute humidity in the range of temperature variation of middle latitudes. This difference in the sensitivity decreases with decreasing temperature. When the temperature is very low, say 240K, the difference is practically negligible, because the mixing ratio of water vapor is extremely small. On the other hand, the equilibrium temperature is very sensitive to the change of the solar constant when the temperature is much above 300K. This result clearly demonstrates the self-amplification effect of water vapor on the equilibrium temperature of the atmosphere with a given distribution of relative humidity. As a reference,

the vertical distributions of equilibrium temperature corresponding to various values of the solar constant are shown in Fig. 8.

b. Outgoing radiation and atmospheric temperature. In order to satisfy the condition of thermal equilibrium, the variation of the solar constant must be compensated for by a corresponding change of the outgoing long-wave radiation at the top of the atmosphere. In this subsection, we shall investigate the dependence of outgoing radiation on atmospheric temperature in order that we may understand the results described just above.

In Fig. 9, various vertical distributions of temperature adopted for the present computations are shown, and in Fig. 10, the upward long-wave radiation at the top of the atmosphere is plotted versus the temperature of the earth's surface T_*. The distribution of relative humidity, cloudiness, and other atmospheric absorbers adopted for this computation are described in Section 2b. In Fig. 9 curves representing blackbody radiation temperatures T_*, (T_*-10), (T_*-20), (T_*-30), and (T_*-50) are also drawn for the sake of comparison. According to this comparison, the outgoing long-wave radiation at the top of the atmosphere with a given distribution of relative humidity depends less upon the atmospheric temperature than is expected from the fourth-power law of Stefan-Boltzmann.

As we explained in the introduction, the deviation from the fourth-power law is mainly due to the dependence of the effective source of outgoing radiation upon the temperature of the atmosphere. This result

explains why the atmosphere with the fixed distribution of relative humidity is more sensitive to the variation of solar radiation than the atmosphere with the fixed distribution of absolute humidity.

4. Equilibrium temperature and atmospheric absorbers

In this section, we shall discuss the dependence of equilibrium temperature upon the vertical distribution of atmospheric absorbers such as water vapor, carbon dioxide, ozone, and cloud. It is hoped that the results of this section will be useful for evaluating the possibility of various climatic changes in the earth's atmosphere.

a. *Tropospheric relative humidity.* In order to evaluate the dependence of equilibrium temperature upon the distribution of relative humidity of the atmosphere, a series of computations of thermal equilibrium was performed for various distributions of relative humidity. The vertical distribution of relative humidity adopted for this series of computations is described by Eqs. (2) and (3), except that we assigned various values to h_*. For the distribution of other gaseous absorbers and clouds, see Section 2b.

Fig. 11 shows the vertical distributions of equilibrium temperature corresponding to h_* values of 0.2, 0.6, and 1.0. The following features are noteworthy.
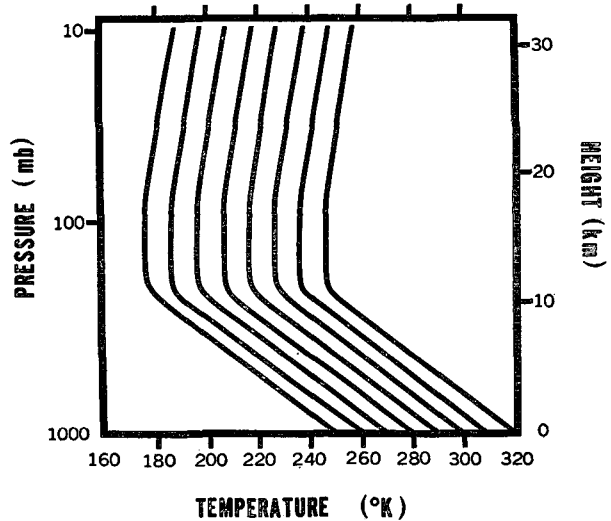

FIG. 9. Vertical distributions of temperature adopted for the computation of radiative flux shown in Fig. 10.

1) The higher the tropospheric relative humidity, the warmer is the equilibrium temperature of the troposphere.
2) The equilibrium temperature of the stratosphere depends little upon the tropospheric relative humidity.

Table 2 shows the dependence of the net upward radiation at the top of the atmosphere R_L, and that
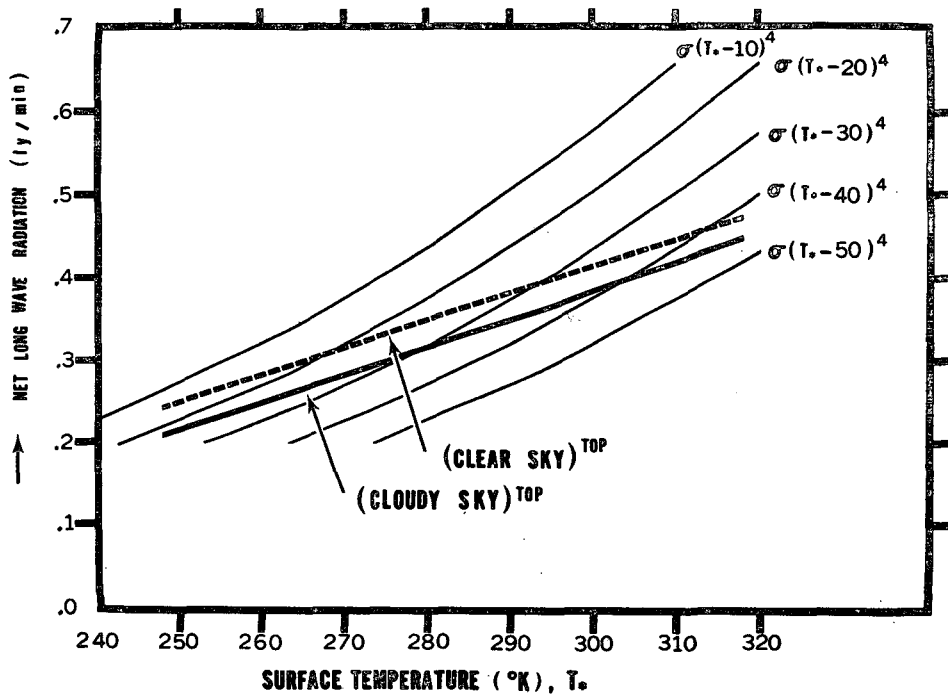

FIG. 10. Net long-wave radiation at the top of the atmosphere for the set of temperature distributions shown in Fig. 9. Thin lines in the background show the black body radiation at the temperatures $(T_* - 10)$, $(T_* - 20)$, $(T_* - 30)$, $(T_* - 40)$, and $(T_* - 50)$.
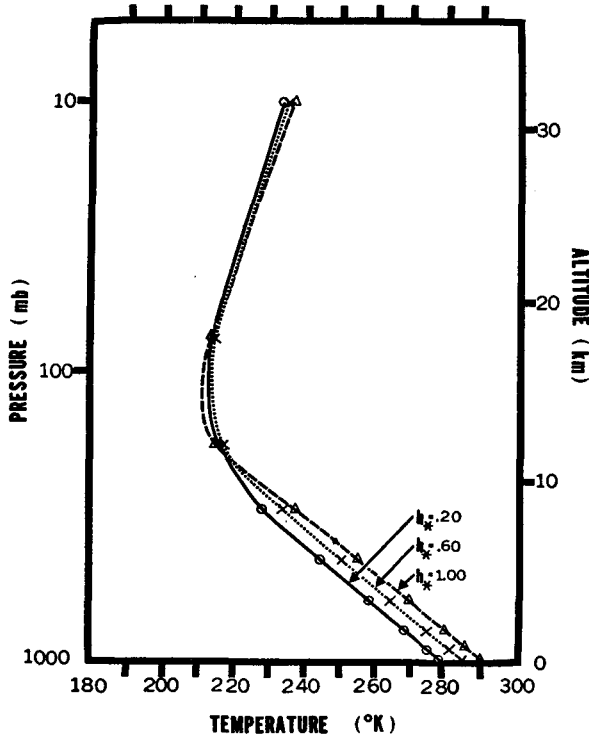
FIG. 11. Vertical distributions of radiative convective equilibrium temperature for various distributions of relative humidity.
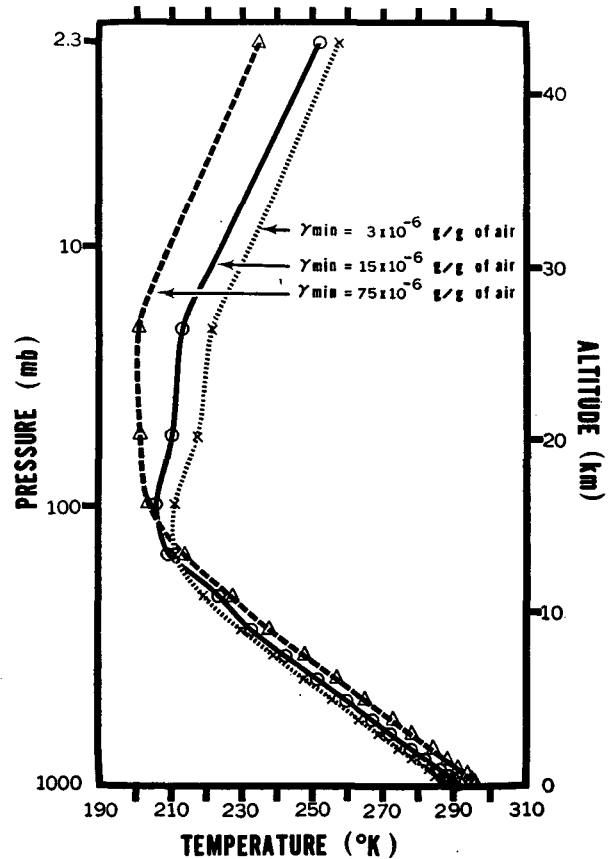

FIG. 12. Vertical distributions of radiative convective equilibrium temperature for various values of water vapor mixing ratio in the stratosphere.

of the surface equilibrium temperature T_*^e upon the relative humidity of the earth's surface. Based upon this table, it is possible to obtain the following approximate relationship between T_*^e and h_*:

$$\frac{\partial T_*^e}{\partial (100 h_*)} \simeq 0.133,$$

the units being degrees Celsius per unit percentage change of relative humidity, and where $1.0 \geq h^* \geq 0.2$. This table also indicates that the net outgoing radiation depends very little upon the tropospheric relative humidity. This is why the dependence of stratospheric temperature upon tropospheric relative humidity is so small.

b. *Water vapor in the stratosphere.* Recently, a panel on weather and climate modification appointed by the National Academy of Science (1966) suggested that the temperature of the earth's atmosphere may be altered significantly by an increase of stratospheric water

vapor anticipated with an increasing number of supersonic transport aircraft flights. It should be useful to evaluate the effect of the variation of stratospheric water vapor upon the thermal equilibrium of the atmosphere, with a given distribution of relative humidity. The distribution of humidity adopted for this series of computations is given by Eqs. (2) and (3), except that the absolute humidity of the stratosphere r_{min} is different for each experiment.

The values of r_{min} chosen for this series of computations are 3×10^{-6}, 15×10^{-6}, and 75×10^{-6} gm gm^{-1} of air. Figs. 12 and 13 show the states of thermal equilibrium thus computed, and the corresponding vertical distributions of water vapor mixing ratio. Examination of Fig. 12 reveals the following features.[1]

1) The larger the stratospheric mixing ratio r_{min}, the warmer is the tropospheric temperature.
2) The larger the water vapor mixing ratio in the stratosphere, the colder is the stratospheric temperature.

TABLE 2. Variation of surface equilibrium temperature T_*^e and net upward radiation at the top of the atmosphere R_L for various values of the relative humidity at the earth's surface h_*.

h_*	T_*^e	R_L (ly min^{-1})
0.2	278.1	0.3214
0.6	285.0	0.3274
1.0	289.9	0.3313

[1] Qualitatively similar conclusions were obtained for the atmosphere with a given distribution of absolute humidity [see M. S. and Manabe and Möller (1961)].

3) The dependence of the equilibrium temperature in the stratosphere upon the stratospheric water vapor mixing ratio is much larger than that in the troposphere.

Table 3 shows the equilibrium temperature of the earth's surface corresponding to various water vapor mixing ratios in the stratosphere. Recent measurements by Mastenbrook (1963) and others suggest that the mixing ratio in the atmosphere is about 3×10^{-6} gm gm^{-1} of air. According to this table, a 5-fold increase of stratospheric water vapor over its present value would increase the temperature of the earth's surface by about 2.0C. It is highly questionable that such a drastic increase of stratospheric water vapor would actually take place due to the release of water vapor from the supersonic transport. Recently, Manabe *et al.* (1965) performed a numerical experiment of the general circulation model of the atmosphere with the hydrologic cycle. They concluded that, in the model atmosphere, the large-scale quasi-horizontal eddies are very effective in removing moisture from the high- and middle-latitude stratosphere by freezing out near the cold equatorial tropopause. Their results must be viewed with caution, however, because their computation involves a large truncation error in evaluating vertical advection of water vapor in the upper troposphere and the lower stratosphere. This study, nonetheless, suggests the

TABLE 3. The variation of the equilibrium temperature of the earth's surface $T_*{}^e$ with stratosphere water vapor mixing ratio r_{min}.

r_{min} (gm gm^{-1})	$T_*{}^e$ (°K)
3×10^{-6}	288.4
15×10^{-6}	290.4
75×10^{-6}	296.0

possible importance of dynamical process in the water balance of the stratosphere.

c. Carbon dioxide. As we mentioned in the introduction, Möller (1963) discussed the influence of the change of CO_2 content in the atmosphere with a given value of relative humidity on the temperature of the earth's surface. He computed the magnitudes of downward long-wave radiation corresponding to various CO_2 contents, and estimated the change of surface temperature required to compensate for the change of net downward radiation due to the change of CO_2 content. His results suggest that the increase in the water content of the atmosphere with increasing temperature causes a self-amplification effect, which results in an almost arbitrary change of temperature at the earth's surface. In order to re-examine Möller's computation by use of the present scheme of computing radiative transfer, the net upward long-wave radiation into the atmosphere with given distributions of relative humidity was computed for various distributions of surface temperature as shown in Fig. 9. The vertical distribution of cloudiness and that of relative humidity have already been specified in Section 2b. In Fig. 14, the magnitude of net radiation thus computed is plotted versus the temperature of the earth's surface. For the sake of comparison, the magnitudes of net flux obtained by using the formulas proposed by Möller (1963), Berliand and Berliand (1952), and Boltz and Falkenberg (1950) are added to the same figure. The relative humidity at the earth's surface needed for these computations is assumed to be 77%. Möller (1963) and Berliand and Berliand (1952) obtained their empirical formulas from radiation chart computations,
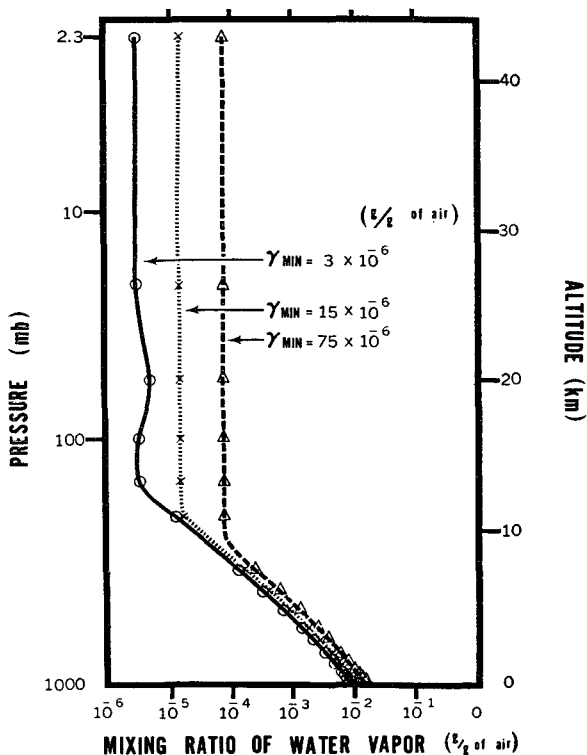

FIG. 13. Vertical distribution of water vapor mixing ratio corresponding to the equilibrium status shown in Fig. 12.
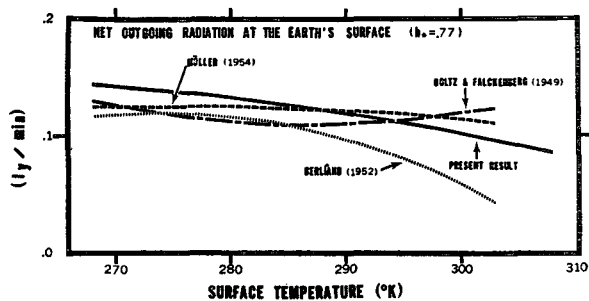

FIG. 14. Values of net upward long-wave radiation at the earth's surface which are computed from the empirical formulas obtained by various authors as well as the values from the present contribution.
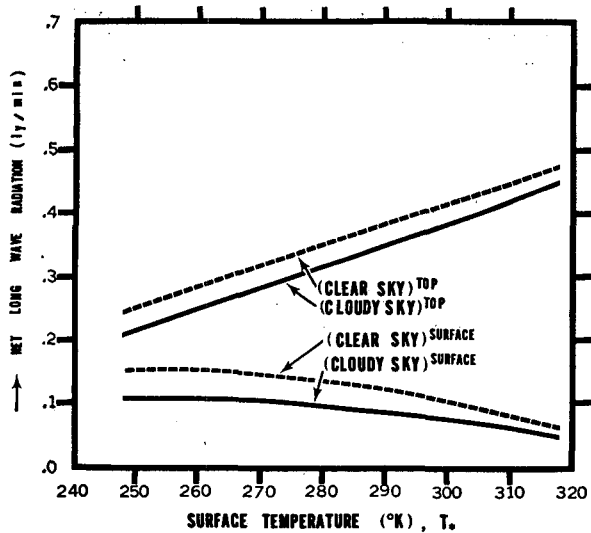
FIG. 15. The net upward long-wave radiation both at the top and bottom of the atmosphere.

TABLE 4. Equilibrium temperature of the earth's surface (°K) and the CO_2 content of the atmosphere.

CO_2 content (ppm)	Average cloudiness		Clear	
	Fixed absolute humidity	Fixed relative humidity	Fixed absolute humidity	Fixed relative humidity
150	289.80	286.11	298.75	304.40
300	291.05	288.39	300.05	307.20
600	292.38	290.75	301.41	310.12

whereas Boltz and Falkenberg (1950) obtained their empirical formula using measurements with a carefully calibrated vibrational pyranometer. Our comparison shows the results obtained by the various methods to be fairly consistent. Generally speaking, the dependence
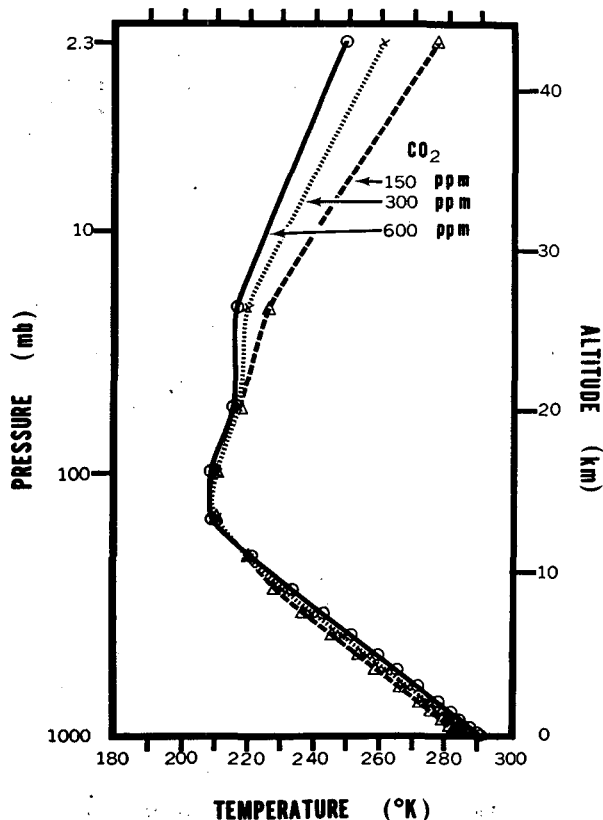
of net radiation upon temperature is small. It increases or decreases with increasing temperature depending upon the method of computation. For example, the results of the present computation and those of Berliand indicate that the net upward radiation decreases monotonically with increasing surface temperature for the ordinary range of temperature. If one discusses the effect of carbon dioxide upon the climate of the earth's surface based upon these results, one could conclude that the greater the amount of carbon dioxide, the colder would be the temperature of the earth's surface, i.e., to compensate for the increase of downward radiation due to the increase of carbon dioxide, it is necessary to have a lower temperature. On the other hand, the result of Boltz and Falkenberg (1950) may lead us to the opposite conclusion for temperatures above 290K. As Möller (1963) suspected, these results do not always indicate the extreme sensitivity of the actual earth's climate. The basic shortcoming of this line of argument may be that it is based upon the heat balance only of the earth's surface, instead of that of the atmosphere as a whole. In Fig. 15, the net upward long-wave radiation at the top of the atmosphere, together with that at the earth's surface, are plotted against the temperature of the earth's surface. As we have already discussed in Section 3b, the former increases significantly with increasing temperature in contrast to the latter. In order to compensate for the decrease of net outgoing radiation at the top of the atmosphere due to the increase of CO_2 content, it is necessary to increase the atmospheric temperature. Therefore, one may expect that the larger the CO_2 content in the atmosphere, the warmer would be the temperature of the earth for the ordinary range of atmospheric temperature. This result is not in agreement with the conclusion which we reached based upon the earth's surface.

FIG. 16. Vertical distributions of temperature in radiative convective equilibrium for various values of CO_2 content.

TABLE 5. Change of equilibrium temperature of the earth's surface corresponding to various changes of CO_2 content of the atmosphere.

Change of CO_2 content (ppm)	Fixed absolute humidity		Fixed relative humidity	
	Average cloudiness	Clear	Average cloudiness	Clear
300 → 150	−1.25	−1.30	−2.28	−2.80
300 → 600	+1.33	+1.36	+2.36	2.92

In order to obtain the complete picture, it is also necessary to consider the effect of convection. Therefore, a series of radiative convective equilibrium computations were performed. Fig. 16 shows the vertical distributions of equilibrium temperature corresponding to the three different CO_2, i.e., 150, 300, and 600 ppm contents by volume. In this figure, the following features are noteworthy:

1) The larger the mixing ratio of carbon dioxide, the warmer is the equilibrium temperature of the earth's surface and troposphere.

2) The larger the mixing ratio of carbon dioxide, the colder is the equilibrium temperature of the stratosphere.

3) Relatively speaking, the dependence of the equilibrium temperature of the stratosphere on CO_2 content is much larger than that of tropospheric temperature.

Table 4 shows the equilibrium temperature of the earth's surface corresponding to various CO_2 contents of the atmosphere, and Table 5 shows the change of surface equilibrium temperature corresponding to the change of CO_2 content. In these tables, values for both the atmosphere with given distribution of absolute humidity, and that with the given distribution of relative humidity are shown together. According to this comparison, the equilibrium temperature of the former is almost twice as sensitive to the change of CO_2 content as that of the latter, but not as sensitive as the results of Möller suggest. These results indicate that the extreme sensitivity he obtained was mainly for the reason already stated.

Although our method of estimating the effect of overlapping between the 15-μ band of CO_2 and the rotation band of water vapor is rather crude, we believe that the general conclusions which have been obtained here on the atmosphere with a fixed relative humidity should not be altered by this inaccuracy. It is interesting to note that the dependencies of surface temperature on the CO_2 content, which were obtained by Möller (1963) and present authors for the atmosphere with a fixed relative humidity, agree reasonably well with each other (see Table 6 for Möller's results).

d. *Ozone.* States of thermal equilibrium were computed for three different distributions of ozone as shown in Fig. 17. These distributions were read off
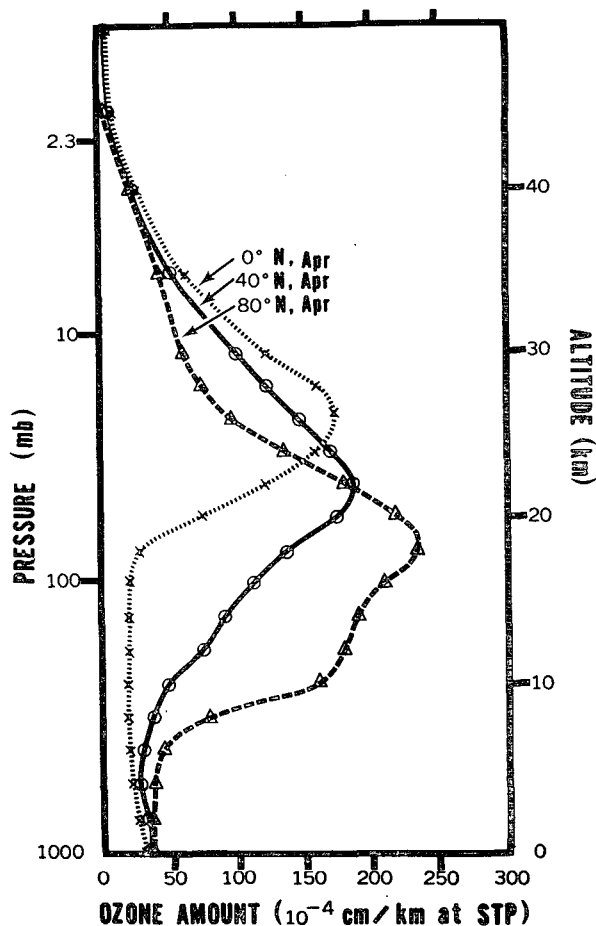

Fig. 17. Vertical distribution of O_3 adopted for the computation of radiative equilibrium shown in Fig. 18. Vertical distribution (Herring and Borden, 1965); total amount (London, 1962).

from the results which were obtained by Herring and Borden (1965), using the chemiluminescent ozonesonde. The total amounts of ozone are adjusted such that they coincide with those obtained by London (1962). Among the three distributions shown in the figure, the total amount for 0N, April, is a minimum, and that for 80N, April, a maximum. Fig. 18 shows the vertical distribution of equilibrium temperature corresponding to each ozone distribution. The following features are noteworthy:

1) The larger the amount of ozone, the warmer is the temperature of troposphere and the lower stratosphere, and the colder is the temperature of the upper stratosphere.

2) The influence of ozone distribution upon equilibrium temperature is significant in the stratosphere, but is small in the troposphere.

3) As we pointed out in M.S., the ozone distribution of 0N, April, tends to make the tropopause height higher and the tropopause profile sharper than those of 80N, April. As reference, equilibrium temperatures of the earth's surface as well as the

TABLE 6. Change of equilibrium temperature of the earth's surface corresponding to various changes of CO_2 content of the atmosphere [computed by Möller using the absorption value of Yamamoto and Sasamori (1958)].

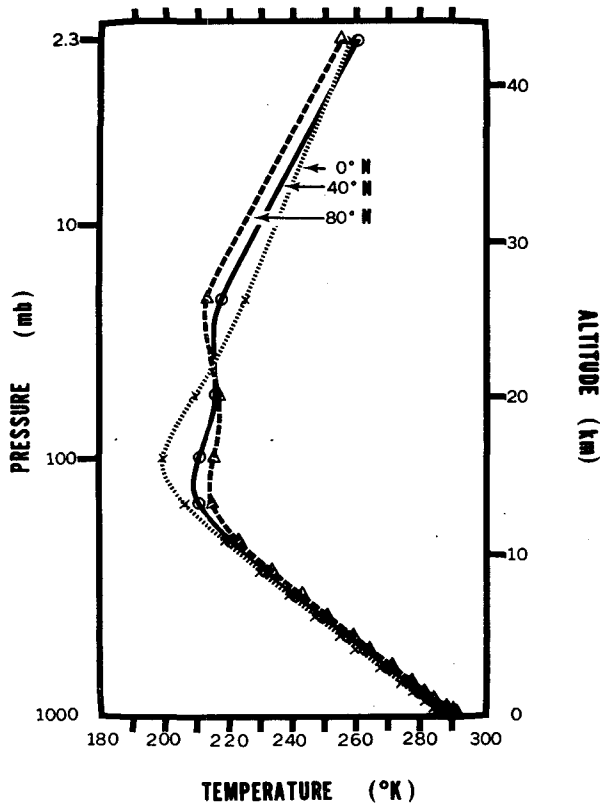| Variation of CO_2 content (ppm)	Fixed absolute humidity	
	Average cloudiness	Clear
300 → 150	−1.0	−1.5
300 → 600	+1.0	+1.5

FIG. 18. Vertical distributions of the temperature of radiative convective equilibrium, which correspond to the ozone distributions shown in Fig. 17.
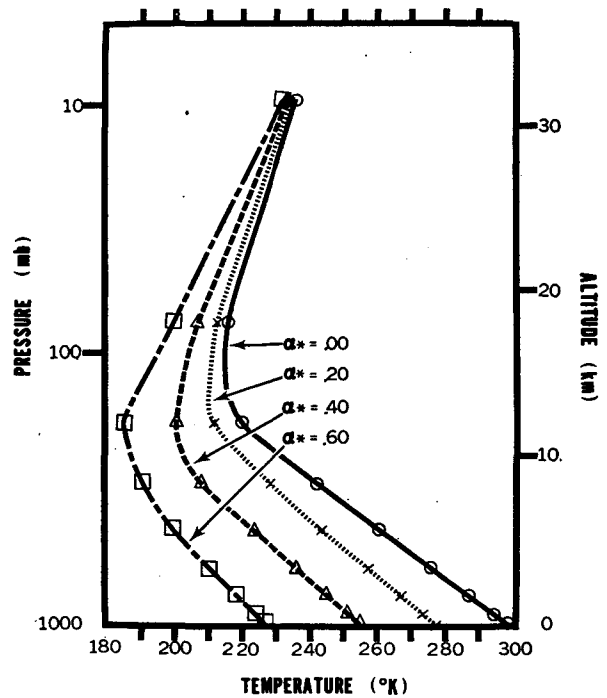

FIG. 19. Vertical distributions of radiative convection equilibrium for various values of surface albedo.

total amounts for the three distributions adopted here are tabulated in Table 7.

e. Surface albedo. A series of thermal equilibrium states of the atmosphere with the given distribution of relative humidity was computed for various albedos of the earth's surface. Fig. 19 shows the results. Examination of this figure reveals the following features:

1) The larger the value of albedo of the earth's surface, the colder the temperature of the atmosphere.
2) The influence of the surface albedo decreases with increasing altitude. It is a maximum at the earth's surface, and is almost negligible at the 9-mb level.

Table 8 shows the surface equilibrium temperature T_*^e for various values of surface albedo α_*. According to this table, the sensitivity of the equilibrium tem-

perature of the earth's surface on the surface albedo may be approximately expressed by

$$\partial T_*^e/\partial(100\alpha_*) = -1,$$

where the units are degrees Celcius change per unit percentage change of surface albedo.

Again, this sensitivity is almost twice as large as that of the atmosphere with a fixed absolute humidity for the ordinary range of solar constant.

f. Cloudiness. A series of thermal equilibrium computations was performed for various distributions of cloudiness. The equilibrium temperatures of the earth's surface for a variety of cloud distributions are tabulated in Table 9 and shown in Fig. 20.

Generally speaking, the larger the cloud amount, the colder is the equilibrium temperature of the earth's surface, though this tendency decreases with increasing cloud height and does not always hold for cirrus. The equilibrium temperature of the atmosphere with average cloudiness specified in the table is about 20.7C colder than that for a clear atmosphere. This difference is significantly larger than the difference of about

TABLE 7. Equilibrium temperatures of the earth's surface for three ozone distributions.

Latitude, month	Total amount O_3 (cm, STP)	T_*^e (°K)
0N, April	0.260	287.9
40N, April	0.351	288.8
80N, April	0.435	290.3

TABLE 8. Surface equilibrium temperatures T_*^e for various values of surface albedo α_*.

Albedo	T_*^e
0.00	297.2
0.20	276.4
0.40	253.2
0.60	227.0

TABLE 9. Effect of cloudiness on surface equilibrium temperature $T_*{}^e$. FB and HB refer to full black and half black, respectively.

Experiment no.	Cloudiness (amount) High	Cloudiness (amount) Middle	Cloudiness (amount) Low	$T_*{}^e$ (°K)
C1	0.000(HB)	0.072(FB)	0.306(FB)	280.1
C2	0.500(HB)	0.072(FB)	0.306(FB)	281.6
C3	1.000(HB)	0.072(FB)	0.306(FB)	284.2
C1	0.000(FB)	0.072(FB)	0.306(FB)	280.1
C4	0.500(FB)	0.072(FB)	0.306(FB)	298.4
C5	1.000(FB)	0.072(FB)	0.306(FB)	318.0
C6	0.218(FB)	0.000(FB)	0.306(FB)	290.5
C7	0.218(FB)	0.500(FB)	0.306(FB)	271.5
C8	0.218(FB)	1.000(FB)	0.306(FB)	251.8
C9	0.218(FB)	0.072(FB)	0.000(FB)	311.3
C10	0.218(FB)	0.072(FB)	0.500(FB)	272.0
C11	0.218(FB)	0.072(FB)	1.000(FB)	229.3
C12	0.000	0.000	0.000	307.8
C13	0.218(FB)	0.072(FB)	0.306(FB)	287.1

13C, which was obtained for the atmosphere with a fixed absolute humidity (see M.S.). The dependence of equilibrium temperature of the earth's surface on the amount of low (C_L) middle (C_M), and high (C_H) clouds may be expressed by the following equations:

$$\partial T_*{}^e / \partial (100 C_L) = -8.2$$

$$\partial T_*{}^e / \partial (100 C_M) = -3.9$$

$$\partial T_*{}^e / \partial [100 C_H(FB)] = +0.17$$

$$\partial T_*{}^e / \partial [100 C_H(HB)] = +0.04.$$

All units are in degrees Celcius change per unit percentage increase in cloudiness. FB and HB refer to full black and half black, respectively.

The reader should refer to Section 2b for the albedo of each cloud type and the distributions of the gaseous absorbers adopted for this computation. Whether
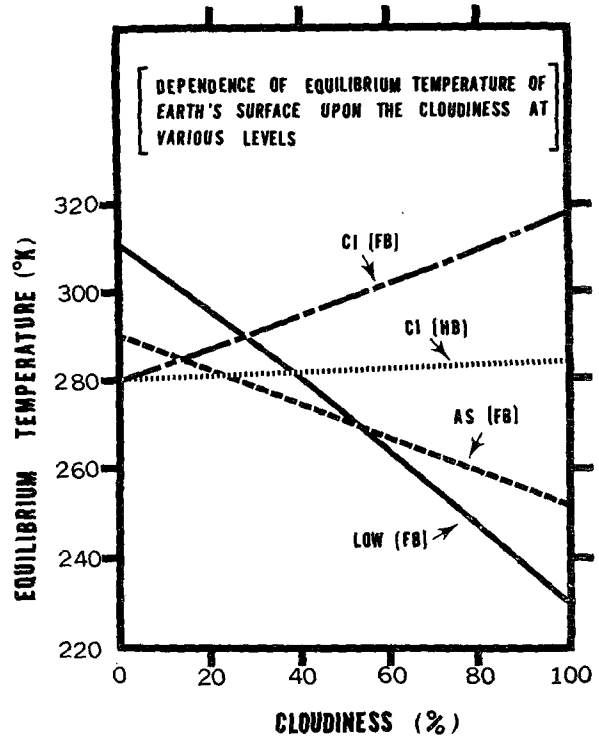

FIG. 20. Radiative convective equilibrium temperature at the earth's surface as a function of cloudiness (cirrus, altostratus, low cloud). FB and HB refer to full black and half black, respectively.

cirrus clouds heat or cool the equilibrium temperature depends upon both the height and the blackness of cirrus cloud. This subject was previously discussed in M.S.

Relatively speaking, the influence of cloudiness upon the equilibrium temperature is more pronounced in the troposphere than in the stratosphere, where the influence decreases with increasing altitude. (Refer to Figs. 21 and 22, which show the vertical distribution of
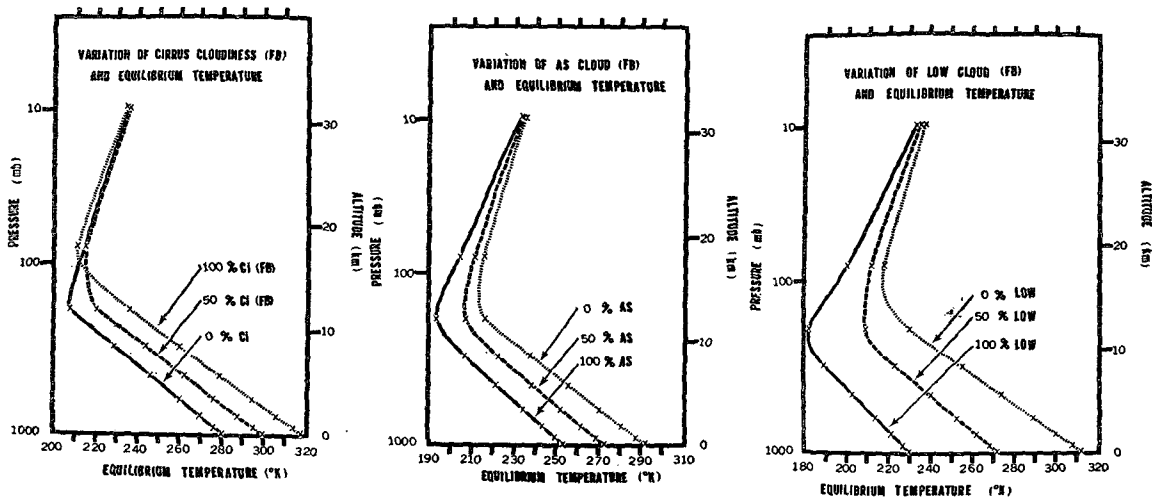

FIG. 21. Vertical distributions of equilibrium temperature for various values of high, middle, and low cloudiness.
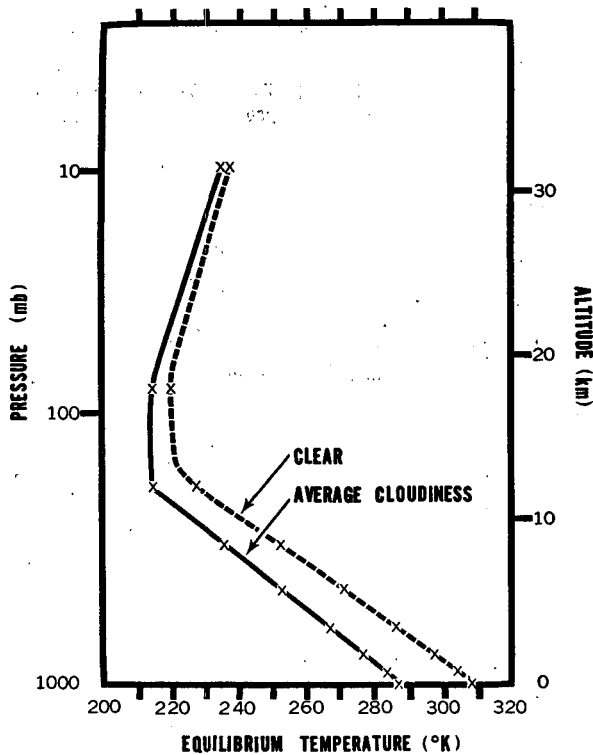
FIG. 22. Vertical distributions of equilibrium temperature for a clear atmosphere and that for an atmosphere with average cloudiness.

equilibrium temperatures for various distributions of cloudiness.) Accordingly, middle and low clouds have a tendency to lower the height of the tropopause.

5. Summary and conclusions

1) A series of radiative convective equilibrium computations of the atmosphere with a given distribution of relative humidity were performed successfully.

2) Generally speaking, the sensitivity of the surface equilibrium temperature upon the change of various factors such as solar constant, cloudiness, surface albedo, and CO_2 content are almost twice as much for the atmosphere with a given distribution of relative humidity as for that with a given distribution of absolute humidity.

3) The speed of approach towards the state of equilibrium is half as much for the atmosphere with a given distribution of relative humidity as for that with the given distribution of absolute humidity. In other words, the time required for radiation-condensation relaxation is much longer than that required for radiation relaxation of the mean atmospheric temperature.

4) Doubling the existing CO_2 content of the atmosphere has the effect of increasing the surface temperature by about 2.3C for the atmosphere with the realistic distribution of relative humidity and by about

1.3C for that with the realistic distribution of absolute humidity. The present model atmosphere does not have the extreme sensitivity of atmospheric temperature to the CO_2 content which Möller (1963) encountered in his study when the atmosphere has a given distribution of relative humidity.

5) A five-fold increase of stratospheric water vapor from the present value of 3×10^{-6} gm gm^{-1} of air causes an increase of surface equilibrium temperature of about 2.0C, when the vertical distribution of relative humidity is fixed. Its effect on the equilibrium temperature of the stratosphere is larger than that of troposphere.

6) The effects of cloudiness, surface albedo, and ozone distribution on the equilibrium temperature were also presented.

Acknowledgments. The authors wish to thank Dr. Smagorinsky and Dr. Möller whose encouragement started this study, Dr. J. Murray Mitchell, Jr., who read the manuscript carefully and who gave us many useful comments, and Mrs. Marylin Varnadore and Mrs. Clara Bunce who assisted in the preparation of the manuscript. Finally, the constant encouragement of Dr. Bryan is sincerely appreciated.

APPENDIX 1

Detail of the Method of Convective Adjustment

Since we did not describe the detail of the method of convective adjustment in M.S., we shall explain the method in this appendix. The following procedures are executed at each timestep (see Fig. 23).
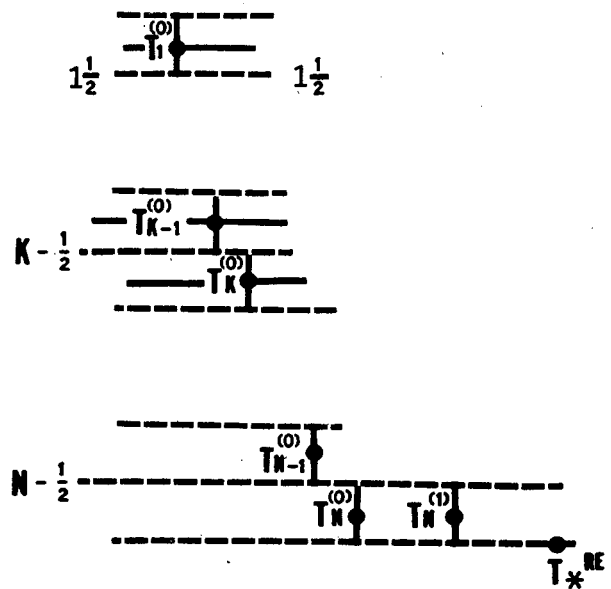

FIG. 23. Notations used for the explanations of convective adjustment.

1) Compute $T_K{}^{(0)}$ ($K=1$, 2, $\cdots$, N) by use of the equation

$$T_K{}^{(0)} = T_K{}^\tau + \left(\frac{\partial T_K{}^\tau}{\partial \tau}\right)_{\text{RAD}} \Delta t,$$

where T_K is the temperature of the Kth level at the τth time step, $(\partial T_K{}^\tau/\partial t)_{\text{RAD}}$ is the rate of change of T_K at the τth time step, and Δt is the time interval of forward time integration.

2) Compute the radiative equilibrium temperature of the earth's surface $T_*{}^{\text{Re}}$ such that it satisfies the relationship

$$(SR)_*{}^\tau + (DLR)_*{}^\tau = \sigma(T_*{}^{\text{Re}})^4,$$

where $(SR)_*{}^\tau$ and $(DLR)_*{}^\tau$ are net solar radiation and downward long-wave radiation at the τth time step, respectively.

3) Compute $T_N{}^{(1)}$ such that it satisfies the relationship

$$C_p\frac{\Delta p_N}{g}(T_N{}^{(1)} - T_N{}^{(0)}) = \sigma\{(T_*{}^{\text{Re}})^4 - (T_N{}^{(1)})^4\}\Delta t,$$

where Δp_N is the pressure thickness of the Nth layer and σ is the Stefan-Boltzmann constant.

4) If $T_N{}^{(1)} - T_{N-1}{}^{(0)} > (LRC)_{N-\frac{1}{2}}$ (unstable), compute $T_N{}^{(2)}$ and $T_{N-1}{}^{(1)}$ such that they satisfy the relationships

$$T_N{}^{(2)} - T_{N-1}{}^{(1)} = (LRC)_{N-\frac{1}{2}},$$

$$C_p\left\{\frac{\Delta p_N}{g}(T_N{}^{(2)} - T_N{}^{(1)}) + \frac{\Delta p_{N-1}}{g}(T_{N-1}{}^{(1)} - T_{N-1}{}^{(0)})\right\}$$
$$= \sigma\{(T_N{}^{(1)})^4 - (T_N{}^{(2)})^4\}\Delta t,$$

where $(LRC)_{N-\frac{1}{2}}$ is the critical (neutral) temperature difference between the Nth and $(N-1)$th level.

If $T_N{}^{(1)} - T_{N-1}{}^{(0)} < (LRC)_{N-\frac{1}{2}}$ (stable),

set $T_N{}^{(2)} = T_N{}^{(1)}$ and $T_{N-1}{}^{(1)} = T_{N-1}{}^{(0)}$.

5) Repeat the following procedures for $K = N-1$, $N-2$, $\cdots$, 1.

If $T_K{}^{(1)} - T_{K-1}{}^{(0)} > (LRC)_{K-\frac{1}{2}}$ (unstable),

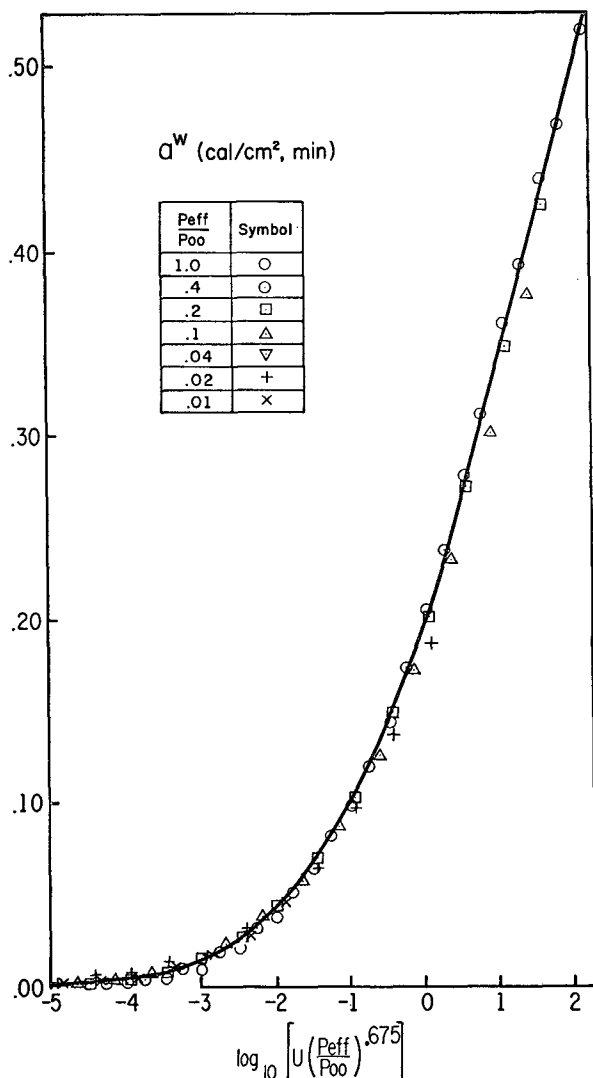compute $T_K{}^{(2)}$ and $T_{K-1}{}^{(1)}$ such that they satisfy

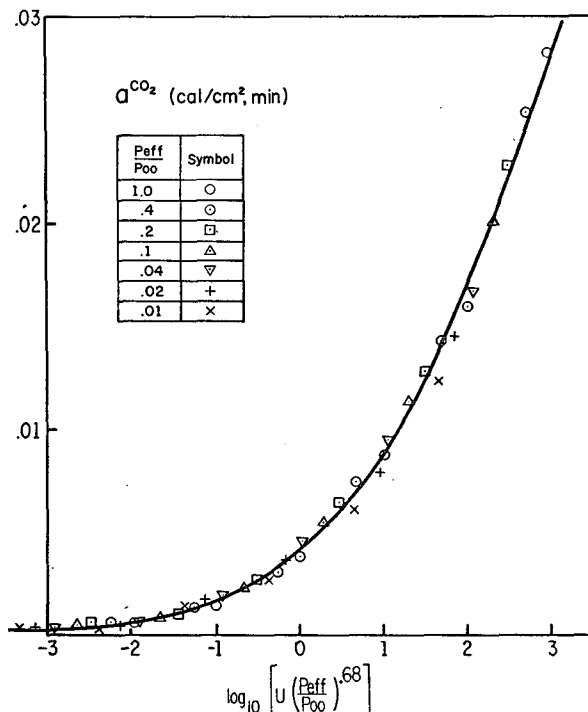FIG. 24. The rate of absorption of solar radiation by H_2O.

FIG. 25. The rate of absorption of solar radiation by CO_2.

the relationships

$$T_K^{(2)} - T_{K-1}^{(1)} = (LRC)_{K-\frac{1}{2}},$$

$$C_p \left\{ \frac{\Delta p_K}{g}(T_K^{(2)} - T_K^{(1)}) + \frac{\Delta p_{K-1}}{g}(T_{K-1}^{(1)} - T_{K-1}^{(0)}) \right\} = 0.$$

6) Repeat processes 4) and 5) after making the following replacement in the equations:

$$T_K^{(n)} \leftarrow T_K^{(n+2)} (K = 1, 2, \cdots, N).$$

7) Repeat process 6) until the layer of supercritical lapse rate is completely eliminated.

Effectively, the temperature of the earth's surface at the $(\tau+1)$th step $(T_*^{\tau+1})$ and that of the atmosphere at the τth step are used for the computation of net radiative flux at the earth's sun face. This method is adopted for the sake of computational stability. Since we reach the final equilibrium which satisfies the requirement described in Section 2a, this inconsistency should not cause any error in the final equilibrium.
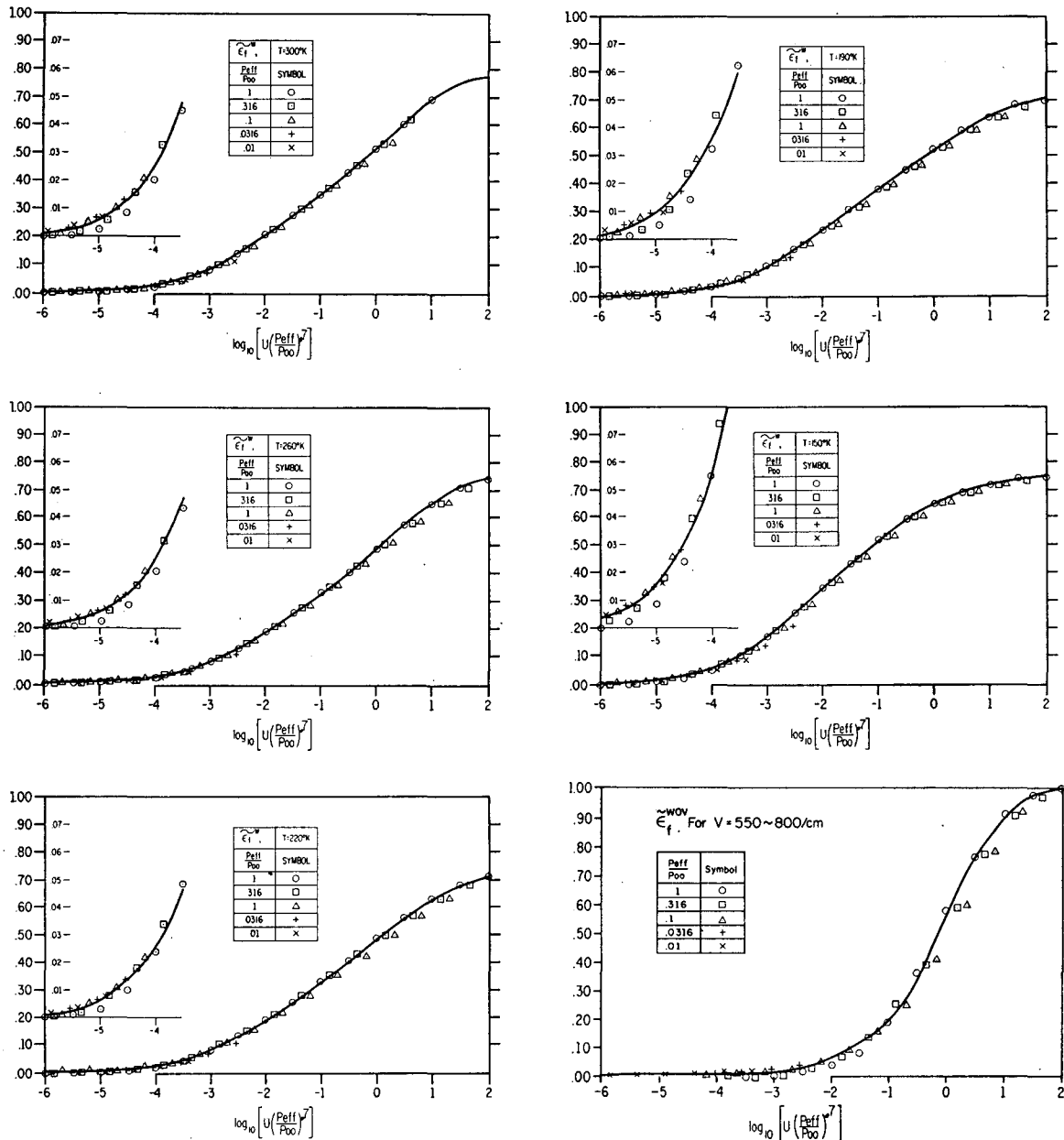

FIG. 26. The mean slab absorptivity of H_2O, from which the contribution of the range of wave number 550–800 cm^{-1} is omitted. In the lower right corner is shown the slab absorptivity of H_2O for the omitted range of wave number.
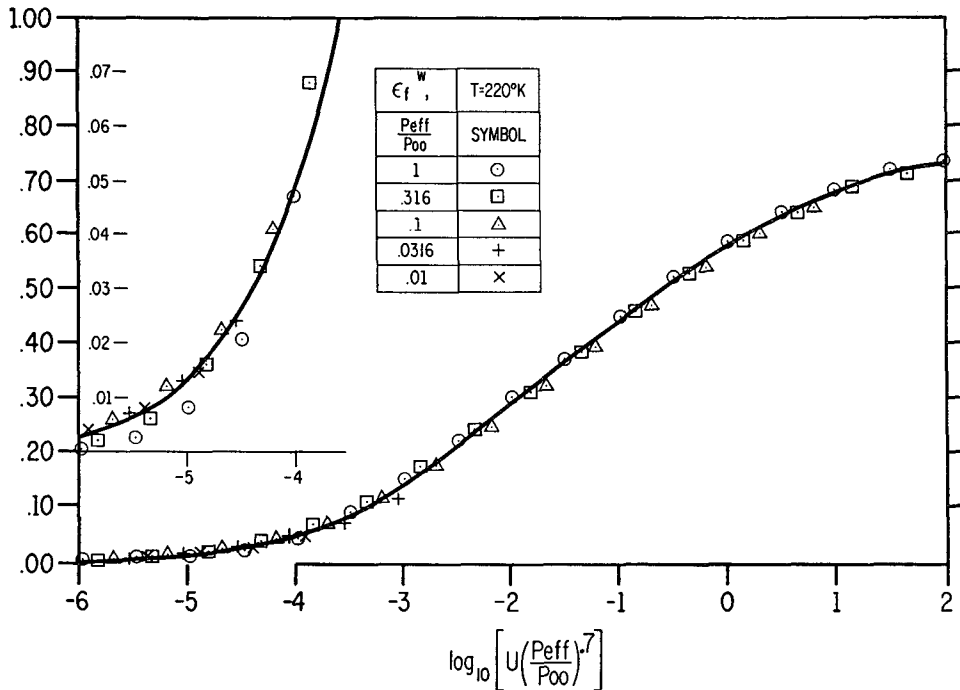
FIG. 27. Emissivity of H_2O from which the contribution of the wave number
range 550–800 cm^{-1} is omitted.

APPENDIX 2

Absorptivities

Absorptivity data, which are used for this study, were given in Figs. A1–A6 of M.S. In these figures, mean slab absorptivities, emissivity, or the rate of absorption of solar insolation were taken as the ordinate,

and the logarithm of optical thickness[2] was taken as the abscissa. The curves which were obtained for various ·pressures using the experimental data are shown in each figure.

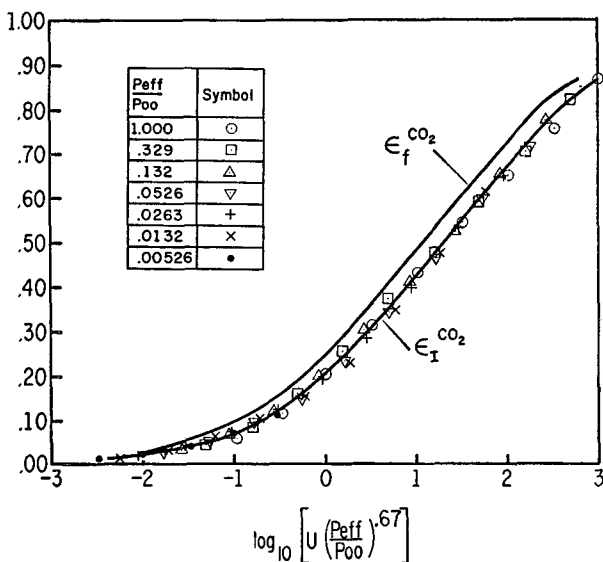As Howard et al. (1955) suggested, one can attempt to parameterize the dependence of the absorptivities

FIG. 28. Slab absorptivity ϵ_f and column absorptivity ϵ_I of CO_2 at 300K. Bandwidth is assumed to be 250 cm^{-1}.
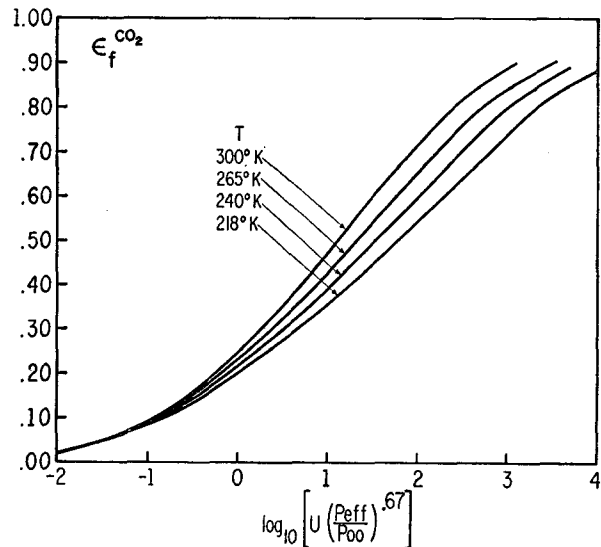

FIG. 29. Slab absorptivities of CO_2 at various temperatures.

[2] In Figs. A1, A2, A3, A4, and A5 of M. S., the abscissas show the logarithm of optical thickness instead of effective optical thickness, which was implied by captions.

TABLE 10. Illustration of the 18-level σ-coordinate system based on $p_* = 1000$ mb. H denotes the approximate height of the level, and Δp is the pressure thickness of the layer.

Level	σ	p (mb)	Δp (mb)	H (km)
1	0.0277	2	9	42.9
2	0.0833	20	25	26.4
3	0.1388	53	40	20.1
4	0.1944	99	52	16.1
5	0.2500	156	62	13.3
6	0.3055	223	71	11.0
7	0.3611	297	77	9.0
8	0.4166	376	81	7.5
9	0.4722	458	83	6.1
10	0.5277	542	83	4.9
11	0.5833	624	81	3.7
12	0.6388	703	77	2.9
13	0.6944	777	71	2.1
14	0.7500	844	62	1.4
15	0.8055	901	52	0.86
16	0.8611	947	40	0.46
17	0.9166	980	25	0.18
18	0.9722	998	9	0.02

upon pressure by taking the following effective optical thickness u_r as abscissa instead of the optical thickness u, i.e.,

$$u_r = (p/p_0)^k u,$$

where p is pressure, p_0 the standard atmospheric pressure, and k the constant to be determined from experimental values. It is not possible, however, to express the absorption curves as a function of u_r alone for the wide range of pressure and optical thickness covered by Figs. A1–A5 of M.S. In order to overcome this difficulty, we limited ourselves to the (p,u) range which is usually needed for the present computation of radiative convective equilibrium of the atmosphere. For example, the combination of a large u and small p or that of small u and large p is not encountered in our computation. This restriction enables us to construct the universal curves which are shown in Figs. 24 or 29. The values of absorptivity which correspond to one-half integral values of the logarithm of optical thickness, are plotted in these figures. However, for the 9.6-μ band only, the values of absorptivity which are obtained from the experiments of Walshaw (1957) are plotted. That part of the (p,u) range which is covered by Figs.

TABLE 11. Illustration of the 9-level σ-coordinate system based on $p_* = 1000$ mb.

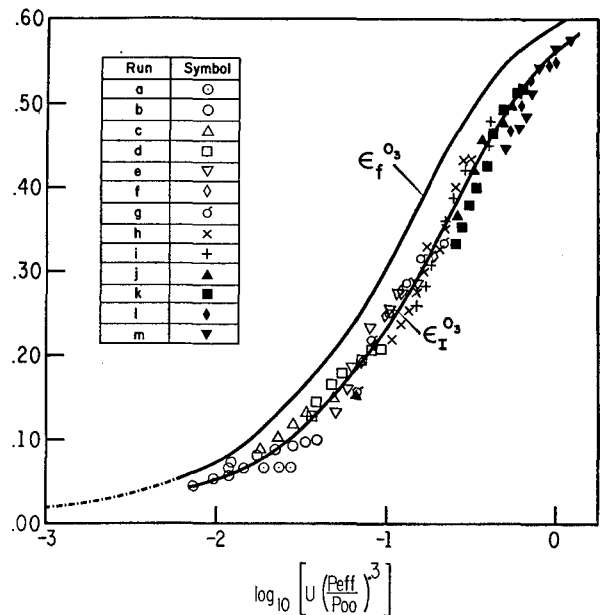| Level	σ	p (mb)	Δp (mb)	H (km)
1	0.0555	9	34	31.6
2	0.1666	74	92	18.0
3	0.2777	189	133	12.0
4	0.3888	336	158	8.3
5	0.4999	500	166	5.5
6	0.6110	664	158	3.3
7	0.7221	811	133	1.7
8	0.8332	926	92	0.64
9	0.9443	991	34	0.07

FIG. 30. Slab and column absorptivity of 9.6-μ band of O_3. Run means the run of experiments by Walshaw (1957). Bandwidth is assumed to be 138 cm^{-1}.

A1–A5 of M.S., but is not encountered in our computation, is omitted from this compilation. Needless to say, it is desirable to use a two parameter u and p. However, one parameter u_r is adopted here for simplicity of programming. On page 368 of M.S. the method of obtaining a^W (Fig. 24) and a^{CO_2} (Fig. 25) are given. Refer to Eq. (13) of M.S. for the definition of $\bar{\epsilon}_f^W$ (Fig. 26), to Eq. (12) of M.S. for the definition of ϵ_f^W (Fig. 27), and to Eqs. (16a), (16b), and (17) of M.S. for the definition of $\epsilon_f^{CO_2}$ (Figs. 28 and 29), $\epsilon_f^{O_3}$ (Fig. 30), and $\bar{\epsilon}_f^{WOV}$ (Fig. 26). For the curve of absorption of solar radiation by ozone, refer to Fig. A6 of M.S.

APPENDIX 3

Both 18 and 9 atmospheric levels are used in the present computations. As in our previous computations, the location of each level is based on a suggestion by J. Smagorinsky. Let the quantity σ be defined as the following function of pressure:

$$Q = p/p_* = \sigma^2(3 - 2\sigma),$$

where p_* is the pressure at the earth's surface and assumed here to be 1000 mb. If we divide the atmosphere into equal σ-intervals, the pressure thickness of the layer is thin both near the earth's surface and the top of the atmosphere. Tables 10 and 11 show the σ-level adopted for 18- and 9-level models, respectively. For our study, we used both 18- and 9-level models.

In order to compare the equilibrium solutions obtained from these two coordinate systems, reference should be made to Fig. 31. The standard distribution of atmospheric absorbers, which is described in Section
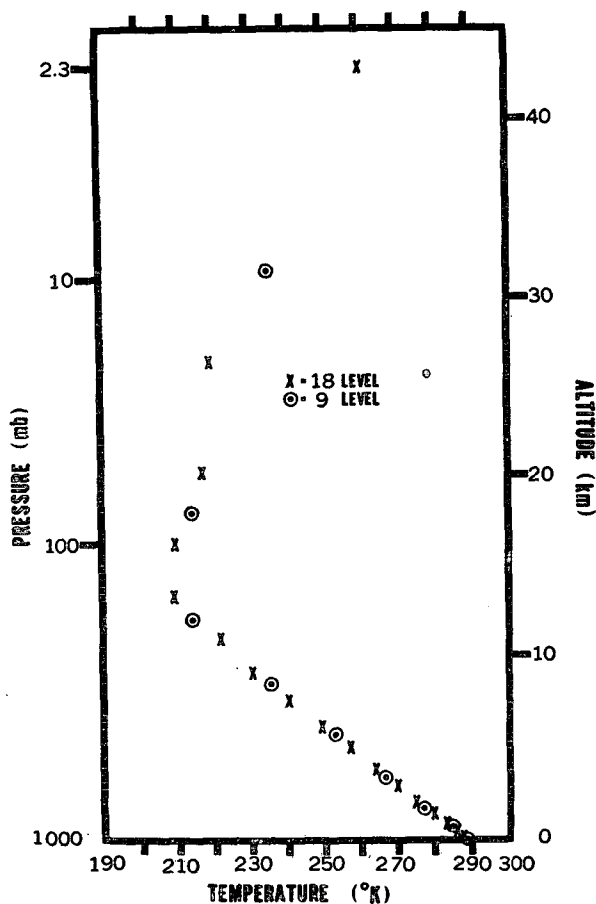
FIG. 31. Radiative convective equilibrium of the atmosphere from the 9- and 18-level models. See text for discussion.

2b is used for both of these computations. The coincidence between the two equilibrium solutions is reasonable.

REFERENCES

Berliand, M. E., and T. G. Berliand, 1952: Determination of the effective outgoing radiation of the earth, taking into account the effect of cloudiness. *Izv. Akad. Nauk SSSR, Ser. Geofiz.*, No. 1, 64–78.

Boltz, H., and G. Falkenberg, 1950: Neubestimmung der Konstanten der Angströmschen Strahlungsformel. *Z. Meteor.*, 7, 65–66.

Hergesell, M., 1919: Die Strahlung der Atmosphäre unter Zungrundlegung bon Lindeberger Temperatur: und Feuchtigkeits Messungen. *Die Arbeiten des Preusslichen Aero-nautischen Observatoriums bei Lindenberg*, Vol. 13, Braunschweig, Germany, Firedr., Vieweg and Sohn, 1–24.

Herring, W. S., and T. R. Borden, Jr., 1965: Mean distributions of ozone density over North America, 1963–1964. Environmental Research Papers, No. 162., AFCRL-65-913, Air Force Cambridge Research Laboratories, Bedford, Mass., 19 pp.

Houghton, J. T., 1963: Absorption in the stratosphere by some water vapor lines in the ν_2 band. *Quart. J. Roy. Meteor. Soc.*, 89, 332–338.

Howard, J. N., D. L. Burch and D. Williams, 1955: Near-infrared transmission through synthetic atmosphere. Geophysics Research Papers, No. 40, Air Force Cambridge Research Center, AFCRC-TR-55-213, 214 pp.

Kaplan, L. D., 1960: The influence of carbon dioxide variations on the atmospheric heat balance. *Tellus*, 12, 204–208.

Kondratiev, K. Y., and H. I. Niilisk, 1960: On the question of carbon dioxide heat radiation in the atmosphere. *Geofis. Pura Appl.*, 46, 216–230.

London, J., 1962: Mesospheric dynamics, Part III. Final Report, Contract No. AF19(604)-5492, Department of Meteorology and Oceanography, New York University, 99 pp.

Manabe, S., and F. Möller, 1961: On the radiative equilibrium and heat balance of the atmosphere. *Mon. Wea. Rev.*, 89, 503–532.

——, J. Smagorinsky and R. F. Strickler, 1965: Simulated climatology of general circulation with a hydrologic cycle. *Mon. Wea. Rev.*, 93, 769–798.

——, and R. F. Strickler, 1964: Thermal equilibrium of the atmosphere with a convective adjustment. *J. Atmos. Sci.*, 21, 361–385.

Mastenbrook, H. J., 1963: Frost-point hygrometer measurement in the stratosphere and the problem of moisture contamination. *Humidity and Moisture*, Vol. 2, New York, Reinhold Publishing Co., 480–485.

Möller, F., 1963: On the influence of changes in the CO_2 concentration in air on the radiation balance of the earth's surface and on the climate. *J. Geophys. Res.*, 68, 3877–3886.

Murgatroyd, R. J., 1960: Some recent measurements by aircraft of humidity up to 50,000 ft in the tropics and their relationship to meridional circulation: *Proc. Symp. Atmos. Ozone*, Oxford, 20–25 July 1959, IUGG Monogr. No. 3, Paris, p. 30.

National Academy of Science, Panel on Weather and Climate Modification, 1966: Weather and climate modification, problem and prospects. Vol II (Research and Development). Publication No. 1350, National Academy of Science—National Research Council, Washington, D. C., 198 pp.

Plass, G. N., 1956: The influence of the 15-micron carbon dioxide band on the atmospheric infrared cooling rate. *Quart. J. Roy. Meteor. Soc.*, 82, 310–324.

Telegadas, K., and J. London, 1954: A physical model of Northern Hemisphere troposphere for winter and summer. Scientific Report No. 1, Contract AF19(122)-165, Research Div. College of Engineering, New York University, 55.pp.

Walshaw, C. D., 1957: Integrated absorption by 9.6 μ band of ozone. *Quart. J. Roy. Meteor. Soc.*, 83, 315–321.

Yamamoto, G., and T. Sasamori, 1958: Calculation of the absorption of the 15 μ carbon dioxide band. *Sci. Rept. Tohoku Univ. Fifth Ser.*, 10, No. 2, 37–57.